Universality, the Barton Nakajima Namikawa relation, and scaling for dispersive ionic materials

J. Ross Macdonald*
Department of Physics and Astronomy, University of North Carolina, Chapel Hill, North Carolina 27599-3255, USA
(Received 27 December 2004; revised manuscript received 10 March 2005; published 27 May 2005)

Many frequency-response analyses of dispersive relaxation for homogeneous glasses, polycrystalline materials, and single crystals involving mobile ions of a single type indicate that estimates of the β_1 shape parameter of the Kohlrausch K1 fitting model are close to 1/3 and are virtually independent of both temperature and ionic concentration. This model, which usually yields better fits than others, including the closely related Kohlrausch K0 one, is indirectly associated with temporal-domain stretched-exponential relaxation having the same β_1 parameter value. Here it is shown that for the above conditions several different analyses all yield a value of 1/3 for the β_1 of the K1 model. It is therefore appropriate to fix the β_1 parameter of this model at the constant value of 1/3, then defined as the U model. It fits data sets exhibiting conductive-system dispersion that vary with both temperature and concentration just as well as the K1 model with β_1 free to vary, and it leads to a correspondingly universal value of the Barton-Nakajima-Namikawa parameter p of 1.65. Composite-model complex-nonlinear-least-squares fitting, including the dispersive U model, the effects of the bulk dipolar-electronic dielectric constant $\varepsilon_{D\infty}$ and of electrode polarization when significant also lead to estimates of two U-model hopping parameters that yield optimum scaling of experimental data involving temperature and concentration variation.

DOI: 10.1103/PhysRevB.71.184307 PACS number(s): 66.30.Dn, 77.22.Gm, 72.20.−i, 66.10.Ed

I. INTRODUCTION

In 1994 Phillips suggested that relaxation in complex (disordered) systems is one of the most important unsolved problem in physics today.[1] Roling and Martiny have recently stated that "Finding an explanation for this high degree of universality (i.e., the existence of master-curves for conductivity isotherms) is still one of the major challenges of solid state physics.[2]" The present work addresses both these challenges. Dyre and Schrøder suggested various macroscopic and microscopic models that predict universality of conduction in the strong-disorder limit.[3] Since universality is an idealized concept, it is not surprising that most claims for universal behavior and models (e.g., Refs. 4 and 5) have been found too limited or even incorrect, but this should not discourage new universality proposals, ones that may still eventually suffer the same fate as new experimental results are analyzed and the domain to which the model is applied is widened.

The principal aim of the present work is to describe a new universal, conductive-system frequency response expression, the U model; define its range of application; and demonstrate its usefulness in fitting and analyzing experimental immittance data. Although this model has evolved from past models, it is both simpler and more general than its precursors. Further, it has been derived from independent macroscopic and microscopic analyses, and it and its three parameters are thus physically well based. Complex-nonlinear-least-squares (CNLS) fitting of dispersive data using the U model allows highly accurate discrimination between bulk ionic response and that associated with electrode effects (see Refs. 6–10 and the present work). Although such effects are usually important in the low-frequency region of experimental data, they may sometimes be non-negligible in the high-frequency region as well.[8]

Since the U model involves temporal stretched-exponential (SE) behavior with a unique value of β_1, it is useful to summarize other related work dealing with SE relaxation (SER). In an earlier paper,[11] both field-free SER in the time domain (for example, in stress relaxation experiments) and field-forced SER in the frequency domain, as in the present work, were discussed. In the former situation, one is concerned with residual relaxation of glasses after initial transients have disappeared, while in the latter the frequency domain is usually limited in practice to frequencies 10^6 times smaller than those involved in atomic vibrations. Field-free data sets are simpler than field-forced ones and are easily fitted by SER. The work of Ref. 11 showed that recent β estimates agreed within ~1% with those predicted by a fractal model in 1996 (Ref. 12), but the field-forced limited data require a much more sophisticated numerical analysis. That model used the concept of fractal dimensionalities to describe the frequency-response behavior in a way that is qualitatively different from the way fractals are used to describe scaling properties near threshold for percolation or near critical points. Readers who are concerned with the fundamental nature of SER and its fractal aspects are encouraged to consult Refs. 11 and 12.

II. DETAILS OF SOME CONDUCTIVE-SYSTEM DISPERSIVE MODELS

A. General expressions

In order to distinguish easily between various fitting models, let the index k take on values of 0 or 1, used in-line or as a subscript. Then for $k=0$, if $\phi_0(t)$ is a conductive-system correlation function, the corresponding normalized frequency response complex function, defined at the complex resistivity level, is[9,13]

$$I_0(\omega) = I_0'(\omega) - iI_0''(\omega) = \frac{\rho_{C0}(\omega) - \rho_{C0}(\infty)}{\rho_{C0}(0) - \rho_{C0}(\infty)} = \int_0^\infty \exp(-i\omega t)\left(-\frac{d\phi_0(t)}{dt}\right)dt, \quad (1)$$

involving a one-sided Fourier transform. Note that a specific expression for the $I_0(\omega)$ response model only follows when one is specified for $\phi_0(t)$, as in the next section. Further, an expression for $\phi_0(t)$ will involve one or more shape parameters which also require specification.

When the small or zero $\rho_{C0\infty} \equiv \rho_{C0}(\infty)$ quantity is neglected as usual,[14] the corresponding $k=0$ frequency response at the complex modulus level is just $M_{C0}(\omega) = M_{C0}'(\omega) + iM_{C0}''(\omega) = i\omega\varepsilon_V\rho_0 I_0(\omega)$. Here the subscript C, used for theoretical and model quantities, denotes conductive-system response and ε_V is the permittivity of vacuum. We shall not distinguish between the $k=0$ and $k=1$ dc resistive quantities $\rho_{C0}(0)$ and $\rho_{C1}(0)$, and will thus use $\rho_0 = 1/\sigma_0$ for either. The quantity σ_0 is the dc limit of the real part of the conductivity, $\sigma(\omega) = \sigma'(\omega) + i\sigma''(\omega) \equiv 1/\rho(\omega)$, where $\rho(\omega) = \rho'(\omega) - i\rho''(\omega)$. The corresponding complex dielectric constant expression is $\varepsilon(\omega) = \varepsilon'(\omega) - i\varepsilon''(\omega) \equiv 1/M(\omega)$.

Consider now the different $k=1$ $I_1(\omega)$ response, closely related to $I_0(\omega)$, as demonstrated in the equation below. When the famous 1973 continuous-time, random-walk (CTRW) approximate microscopic model of Scher and Lax[15] is extended slightly to make its imaginary part fully consistent with its real part at the complex conductivity level,[14] this conductive-system hopping model may be expressed most simply at the complex modulus level as.[9,14,16]

$$M_{C1}(\omega) = M_{C1}'(\omega) + iM_{C1}''(\omega) = i\omega\varepsilon_V\rho_0 I_1(\omega) \equiv [1 - I_{01}(\omega)]/\varepsilon_Z, \quad (2)$$

where the important effective-dielectric-constant quantity ε_Z is defined as $\varepsilon_{C1}'(\infty) \equiv \varepsilon_{C1\infty} = 1/M_{C1}(\infty)$ and the 01 subscript in Eq. (2) indicates that $I_{01}(\omega)$ is of the form of $I_0(\omega)$, but it involves $I_1(\omega)$ fit parameter values rather than those obtained by direct fitting of the same data with the $k=0$ $I_0(\omega)$ model. In Ref. 15, the $\phi_0(t)$ correlation function that leads to the $I_0(\omega)$ normalized frequency response is defined as the probability that a hopping entity remains fixed in place over the time interval from 0 to t.

Equation (2) provides a direct connection between the different $I_1(\omega)$ and $I_0(\omega)$ responses, but the time domain response $\phi_1(t)$ directly following from $I_1(\omega)$ is not of the same form as that of $I_0(\omega)$.[11,14] Importantly, Eq. (2), arising from a detailed microscopic analysis, is, however, of exactly the same form as that derived macroscopically, contemporaneously, and independently by Moynihan, Boesch, and Laberge[17] by considering electric field decay at constant dielectric displacement. This formal micro-macro agreement for the $k=1$ model, unique among dispersive conductive-system response models, thus provides additional justification for it. It remains general, however, until specific forms of $\phi_{01}(t)$ and ε_Z are introduced. Here $\phi_{01}(t)$ is the $k=0$ correlation function that leads to $I_{01}(\omega)$ through Eq. (1) and then to the $k=1$ $I_1(\omega)$ response from Eq. (2). Thus $\phi_{01}(t)$ is the effective correlation function leading to $I_1(\omega)$ and it will involve the same form as $\phi_0(t)$, but a different shape parameter value.

It follows from the work of Scher and Lax,[15] Eq. (2), and Refs. 6–9, 14, and 18 that for the general present $k=1$ dispersion model the very important quantity $\varepsilon_Z = \varepsilon_{C1\infty}$ may be expressed as

$$\varepsilon_{C1\infty} = (\sigma_0/\varepsilon_V)/\langle\tau^{-1}\rangle_1 \equiv \varepsilon_{Ma}/\langle x^{-1}\rangle_1 = \varepsilon_{Ma}\langle x\rangle_{01} = [\gamma N(qd)^2/(6k_B\varepsilon_V)]/T, \quad (3)$$

a purely conductive-system quantity. Here $x \equiv \tau/\tau_0$, τ_0 is a characteristic relaxation time for the model that determines the placement on the frequency scale of the model response, $\varepsilon_{Ma} \equiv \sigma_0\tau_0/\varepsilon_V$, and $\langle\tau^{-1}\rangle_1$ and $\langle\tau\rangle_{01} \equiv \tau_0\langle x\rangle_{01}$ are different averages over the $k=1$ and $k=0$ distributions of relaxation times, respectively. When the form of $\phi_0(t)$ is known, one can calculate $\langle\tau\rangle_0$ from $\langle\tau\rangle_0 = \int_0^\infty \phi_0(t)dt$ (Refs. 13 and 15) and a similar equation applies with the $k=0$ subscripts replaced by 1. Although the $\phi_1(t)$ temporal-response function can be calculated numerically from the $k=1$ distribution of relaxation times,[13,16] it is not needed here in order to obtain an expression for $\langle\tau\rangle_1$. When both the $k=0$ and $k=1$ distributions involve the same value of the shape parameter, as denoted in Eq. (3) by the 01 subscript, they are closely related, yielding the normalized relation $\langle x^{-1}\rangle_1 = 1/\langle x\rangle_{01}$ used in Eq. (3).[6,16] Equation (3) is consistent with the Scher-Lax result that ρ_0 is proportional to $\langle\tau\rangle_{01}$, identified in their work as the mean waiting time for a typical hop,[14,15,18] a physically plausible result.

The quantity N is the maximum mobile charge number density, γ is the fraction of charge carriers of charge q that are mobile, d is the rms single-hop distance for a hopping entity, and k_B is the Boltzmann constant. The high-frequency-limiting effective dielectric constant $\varepsilon_{C1\infty}$, associated entirely with mobile-charge effects, is likely to arise from the short-range vibrational and librational motion of caged ions. The CTRW microscopic analysis of Scher and Lax[15] does not include a maximum transition rate, and so its relaxation-time distribution is not cut off. Numerical analysis shows, however, that a cutoff at the plausible value of 1 ps has a negligible effect on the value of $\varepsilon_{C1\infty}$ in the usual experimental frequency range. Further, when the accurate U-model $\varepsilon_{C1}''(\omega)$ response was inverted to estimate its distribution and then that distribution employed to calculate the associated $\varepsilon_{C1}'(\omega)$ response, the latter showed a clear approach to a constant limiting value of $\varepsilon_{C1\infty}$ (Ref. 14). Therefore, it is clear that a nonzero value of $\varepsilon_{C1\infty}$ is an intrinsic consequence of both the macroscopic and microscopic analyses yielding the K1 response, although nonzero but small values of the limiting quantity $\rho_{C0\infty}$ cause $\varepsilon_{C1}'(\omega)$ to approach zero at sufficiently high frequencies.[14]

In addition to $\varepsilon_{C1\infty}$, a bulk high-frequency-limiting dielectric constant $\varepsilon_{D\infty}$, associated with nondispersive dipolar and vibratory effects of the elements of the basic material, is always present. Thus, for an appreciable range of high

frequencies,[14] the total limiting dielectric constant is $\varepsilon_\infty = \varepsilon_{C1\infty} + \varepsilon_{D\infty}$. Although the important quantity $\sigma'(\omega)$ approaches a final plateau at sufficiently high frequencies,[14] we shall be concerned here only with high-frequency behavior occurring before the effects of the plateau become important, the usual experimental situation.

Because of the endemic presence of $\varepsilon_{D\infty}$, a quantity not directly associated with mobile-charge effects, it is necessary in fitting data to always include a free dielectric parameter in the fitting model, ε_x, to represent ε_∞ for $k=0$ or $\varepsilon_{D\infty}$ for $k=1$ situations, as discussed in the following section. Two fitting parameters present in all the following models are ρ_0, a quantity that determines the magnitude or scale of the response, and τ_o, defined above.

B. Specific models associated with stretched-exponential temporal response: K0, K1, and U

1. Stretched-exponential temporal response, the K0 frequency-response model, and electrode effects

As already mentioned, an explicit expression for $\phi_0(t)$ is required in order to calculate specific $k=0$ and $k=1$ frequency responses for data fitting or data simulation. The $k=0$ choice leads to the K0-model response when the ubiquitous stretched-exponential relation $\phi_0(t) = \exp\{-(t/\tau_o)^{\beta_0}\}$ with $0 < \beta_0 \leqslant 1$ (Refs. 1, 11, 12, 19, and 20), originally introduced by Kohlrausch, is used in Eq. (1) to obtain an explicit expression, or numerical representation, for $I_0(\omega)$. Then, such results may be used to calculate the K0-model modulus-level frequency response $M_{C0}(\omega) = i\omega\varepsilon_V\rho_0 I_0(\omega)$ (Refs. 6–11). Next, Eq. (2) leads to the K1-model frequency response.[7,9,11,21] Here β_0 is both the stretching factor in the time domain as well as the parameter that determines the shape of the K0-model frequency response. The corresponding K1 shape parameter, unequal to β_0, is defined as β_1 and appears in the SE expression for $\phi_{01}(t)$. Although both the K0- and K1-model responses must actually be calculated numerically for arbitrary β_k values, the free LEVM CNLS computer program allows the parameters of these models to be very accurately determined for both data fitting and simulation tasks.[22]

Unlike the K1 model, which involves the nonzero high-frequency-limiting effective dielectric constant $\varepsilon_{C1\infty}$ of Eq. (3), the conductive-system K0 response involves no such limiting value and so $\varepsilon'_{C0}(\infty) = 0$.[6,9] But for experimental data that are well fitted by the K1 model, the actual total high-frequency-limiting dielectric constant implicit in the data is $\varepsilon_\infty = \varepsilon_{C1\infty} + \varepsilon_{D\infty}$, and it will be this value, rather than just $\varepsilon_{D\infty}$, that is estimated by the ε_x free parameter that must be included in fitting using the K0 model. Such a composite model has been designated the CK0, where the "C" here represents the capacitance associated with ε_x (Refs. 7 and 9).

For most data situations, one should also include in a composite fitting model a separate electrode-effects model in series with that representing bulk conductive-system dispersion. The electrode model should represent the effect of partial or complete blocking of mobile charges at the electrodes. Surprisingly, it has been shown that such effects can sometimes be important at high frequencies, as well as at the low-frequency end of the data range.[8] Since electrode effects may thus appreciably influence experimental data, as demonstrated in Sec. III B below as well as in Ref. 8, it is important to initially include this possibility in a composite fitting model and evaluate the need for such inclusion.

In recent work,[6,7,9,11] CNLS fitting results, using several different Kohlrausch and other fitting models, with and without electrode-effect model contributions, have been compared using experimental data for glasses, polycrystalline materials, and single crystals. The inclusion of electrode effects led to important improvements in the fit accuracy for most of the model fits, particularly for the best-fit K0 and K1 ones. Further, for K1 fits without such inclusion estimates of $(1-\beta_1)$ were sometimes as small as 0.5, but increased to very close to 0.67 when such effects were included. Even when not mentioned explicitly in the following work, it should be understood that the fits of experimental data sets discussed herein included not only a bulk-dispersion model such as the K1 or U one, but also a series electrode-model contribution when needed.

2. Two different K1 models

a. Original-modulus-formalism fitting model. The widely used pioneering treatment of Ref. 17, now termed the original modulus formalism (OMF) approach and involving the $k=1$ K1 response model defined in Eq. (2), is unfortunately critically flawed by its improper identification of the ε_Z of Eq. (2) as $\varepsilon_\infty \equiv \varepsilon'(\infty)$, a quantity that includes all contributions to the high-frequency-limiting dielectric constant.[11,21] Since the authors did not recognize the existence of $\varepsilon_{C1\infty}$, their ε_∞ was considered to be just $\varepsilon_{D\infty}$, rather than $\varepsilon_\infty = \varepsilon_{C1\infty} + \varepsilon_{D\infty}$. In the usual case where both quantities are nonzero, data fitting would yield an estimate of $\varepsilon_x = \varepsilon_\infty$, identified as $\varepsilon_{D\infty}$, but actually including both contributions to ε_∞. The failure to distinguish between these two quantities by not including a separate fit parameter such as ε_x leads to an inappropriate mixing of dipolar dielectric effects and those associated only with mobile charge, and thus to both theoretical and experimental inconsistencies, especially in the estimation of β_1 (Refs. 7, 9, and 21). In particular, fits with data expressed at the $M''(\omega)$ level yield quite different estimates of β_1 than those of $\sigma'(\omega)$ for the same data.[21]

Many hundreds of published data fits and analyses since 1973 of $M''(\omega)$ data using the OMF, and thus the K1 model alone, have yielded strong dependence of the estimated β_1 values on ionic concentration and appreciable temperature dependence as well. For example, as the ionic concentration approaches zero, the OMF fits lead to β_1 estimates that approach unity (e.g., Ref. 23). This is because then $\varepsilon_{C1\infty} \to 0$, $\varepsilon_\infty \to \varepsilon_{D\infty}$, and true dispersive effects become more and more negligible compared to Debye-type relaxation involving only σ_0 and $\varepsilon_{D\infty}$, a response that necessarily involves a β value of unity. It is clear that all OMF fits should be fully discounted and such fitting replaced by a consistent approach such as the corrected modulus one described below.

b. Corrected-modulus-formalism approach. The corrected modulus formalism (CMF) also uses the K1 model, but includes a free ε_x parameter, therefore denoted the CK1 model.

For this model, $\varepsilon_x = \varepsilon_{D\infty}$ because $\varepsilon_{C1\infty}$ is not a free parameter of the fit and is completely determined, as in Eq. (3), by the estimates of the K1-model parameters σ_0, τ_0, and β_1. It has been found that CK1 fits for a variety of materials, ionic concentrations, and temperatures lead to virtually constant estimates of β_1, all very close to a value of $1/3$, along with both better fitting and no inconsistencies.[6–9,11,21]

Let us temporarily replace the symbol β_1 by β_{1C} to distinguish it from a β_1 obtained from OMF fitting. Then for the K1 model with $\varepsilon_Z = \varepsilon_{C1\infty}$ in Eq. (2), Eq. (3) may be expressed as

$$\varepsilon_{C1\infty} = \varepsilon_{Ma}\langle x\rangle_{01} = \varepsilon_{Ma}\beta_{1C}^{-1}\Gamma(\beta_{1C}^{-1}) = A/T, \tag{4}$$

appropriate for CK1 fits. This equation applies when cutoff of the K1 distribution of relaxation times is either absent or negligible. Here A is the term in square brackets at the right-side end of Eq. (3) and depends on the ionic concentration, but not usually on the temperature,[7] $\Gamma\cdots$ is the Euler gamma function, and β_{1C} is a value of β_1 obtained from fitting using the CMF with the separate free parameter ε_x to estimate $\varepsilon_{D\infty}$. It follows from Eq. (4) that when A is temperature independent, the thermally activated quantities $T\tau_0$ and τ_0 each exhibit Arrhenius behavior and their product is itself temperature independent.

3. The U model and some of its consequences

a. β_1 derivations. The U model, a simplification of the corrected modulus formalism approach, is particularly important both because of its simplicity (only two free parameters) and because of its universal character over a wide (but still limited) domain of applicability. It is defined as a Kohlrausch K1 model in which the important shape parameter β_1 is fixed at the nonarbitrary, required value of $1/3$, as discussed below. In practice, it will represent the conductive-system dispersive-model part of a composite fitting model that includes not only $\varepsilon_{D\infty}$, but also a part that accounts for electrode effects when important.

The U model applies only to materials that are microscopically homogeneous with respect to density and composition. Such materials should allow conduction in all three dimensions and involve mobile charge carriers of a single type.[11] Only materials and data satisfying these conditions are discussed here for U-model applications. Fitting results with the CK1 model and β_1 taken free to vary may be expected not to satisfy one or more of these criteria when the estimate of β_1 is appreciably different from $1/3$ and is not limited by a very small available frequency range. An experimental finding of β_1 close to $1/3$ for materials with mobile charge carriers of a single type may be taken, however, as an indication that the materials are homogeneous in the present sense.

Some further clarification of the homogeneity requirement that leads to the present kind of universality is worthwhile since it has been found present, by the above definition, for examples of glasses, single crystals, and polycrystalline materials. For glasses and deeply supercooled ionic melts, microscopic homogeneity is necessary.[11,12] Amorphous materials are not usually homogeneous, and for single crystals to qualify for the present universality class, they should be uniformly pervaded by strongly interacting native defects, such as oxygen vacancies. Finally, for polycrystalline materials the bulk crystallites should also contain homogeneously distributed defects, and analysis should account separately for grain-boundary and electrode effects when significant.

In earlier work, data fitting with either the original or corrected modulus formalism, both of which involve the K1 model, has involved a β_1 parameter usually taken free to vary and therefore determined by the fit estimate. Such analyses suggest either no physical explanation of β_1 values or they have been improperly interpreted, on the basis of inappropriate original-modulus-formalism fit results,[21] as a concentration-dependent measure of correlation between hopping ions (e.g., Ref. 24). It is therefore of great importance to provide an experimentally and physically based justification for the present fixed value of $1/3$, one that is not interpreted as associated with such variable ion-ion correlation. Three different approaches are presented below. The U model is the only one available for fitting conductive-system data that is supported by both macroscopic and microscopic analyses and involves a nonarbitrary and well-defined shape parameter.

i. Experimental. Define n, n_0, and n_1 as the high-frequency-limiting log-log slopes of $\sigma'(\omega)$ for data and for the K0 and K1 models, respectively. Data fitting and analysis show that these quantities are closely frequency independent for sufficiently high frequencies in the absence of nearly constant loss and high-frequency electrode effects, and so they are the exponents of power-law responses. Thus, fitting in such a high-frequency region with a power-law model is appropriate for determining n. Good fits of $\sigma'(\omega)$ experimental and synthetic data extending to sufficiently high frequencies indeed show that all three of these slopes are equal as they should be, and for materials satisfying the present U-model criteria n has been frequently found to be very close to $2/3$ in value for many different glasses.[25–27]

Fitting estimates of β_0 and β_1 using the CK0 and CK1 models lead to $\beta_0 = n_0 = n$ and to $1-\beta_1 = n_1 = n$ when the data include an appreciable high-frequency response. The usual relation[9,14] $1-\beta_1 = \beta_0$ follows immediately. When the limiting slopes are $2/3$, it follows that $\beta_0 = 2/3$ and $\beta_1 = 1/3$, the value used in the U model. Therefore, it seems likely that the U model would be most appropriate for fitting all data for which $n \approx 2/3$.

ii. Hopping theory. Although Phillips[1,12] has treated stretched-exponential relaxation in great detail, his work primarily considered mechanical and dielectric relaxation results for nonconductors, with little consideration of β_1 estimates obtained from data involving frequency dispersion associated with mobile charge carriers under field-forced conditions. As he discusses, however, several treatments of the trapping model involving fixed trapping sites lead to the result

$$\beta = d_e/(2 + d_e), \tag{5}$$

where d_e is the effective dimensionality of the configuration space in which dispersive effects occur.

For Coulomb interactions, the value $d_e = 3/2$ was derived, leading to $\beta = 3/7$, while for spin glasses on cubic lattices a

value of $1/3$ was obtained with $d_e=1$. The spin-glass model is not directly appropriate for the present situation, and the maximum-disorder universal-model treatments of Dyre and Schrøder[3] do not involve explicit Coulomb effects. A value of $d_e=1.35$ was found to be most appropriate by these authors. Further, there is no reason to believe that the stretched-exponential correlation function $\phi_0(t)$, with $0<\beta_0\leqslant 1$, necessarily includes such effects.

The U model is consistent with a value of $d_e=1$ when Eq. (5) is applicable. Some implications of the above results are as follows. The Scher-Lax stochastic model, the microscopic basis for the K1 and U models,[15] is a three-dimensional (3D) one that treats all sites on a discrete lattice as equivalent and independent and leads to a frequency response substantially different from that of a later on-off one-dimensional bond-percolation stochastic model.[28,29] Thus, while the $\beta_1=1/3$ value does not directly imply that the motion of the hopping charge carriers is always one dimensional, it does imply that the SE correlation function determining the K1 response, $\phi_{01}(t)$, is associated with a waiting-time distribution best interpreted in terms of correlated processes occurring in a configuration subspace with an effective dimension of unity. In contrast, if Eq. (5) were applied directly to the K0 model, then the $\beta_0=2/3$ value would be associated with an unlikely effective dimensionality of 4. These conclusions raise the need for a detailed microscopic treatment that justifies the U-model requirement that the effective dimensionality of its ion-ion correlation function be unity.

Although a recent geometric derivation of stretched-exponential response for mobile charge carriers leads to a continuously variable β (Ref. 30) and so is not relevant to the present results, a much earlier CTRW treatment,[19,20] involving some elements of the Scher-Lax equation (2) model derivation, showed that the value of β in stretched-exponential temporal response was determined by the rate at which mobile defects find new sites where dipole orientation then relaxes. Although this defect-diffusion model involved dielectric dispersion and dipolar reorientation, it may be applied to the present case of conductive-system dispersion associated with mobile charges. It then shows that for one-dimensional motion the value of β_0 is half that for three-dimensional diffusion, so $\beta_0(3)=2\beta_0(1)$. The corresponding $I_0(\omega)$ frequency responses involving the K0 model should also satisfy this relation, as should their associated SE $\phi_0(t)$ correlation functions, but not the corresponding K1-model quantities not directly involving SER.

Although the dimensionality of a hopping material is an intrinsic property of it, its effective dimensionality also depends on material structure and external factors, such as the presence or absence of a uniaxial forcing field. One therefore needs to consider both the actual dimensionality of the material and its effective dimensionality in considering appropriate values for β_0 and β_1 for different dimensionalities. In particular, the effective dimensionality of the configuration subspace for mobile charge correlations, and so that of their correlation function, is not necessarily the same as the pertinent d value.

For the usual field-forced situation, both experimental results, discussed in the preceding section, and theoretical ones, presented in the following section, show that for the K0 model, $\beta_0(3)=2/3$ is a well-justified choice. It then follows from the above defect-diffusion-model expression that $\beta_0(1)=1/3$, a value also consistent with the limited experimental frequency-response data currently available for $d=1$ situations and with the topological approach of the next section. Because of the equality of the high-frequency log-log $\sigma'(\omega)$ slopes for the $d=3$ and $d=1$ K0 and K1 models, as further demonstrated in Sec. III C, we may write $\beta_1(d)=1-\beta_0(d)$, and so $\beta_1(3)=1/3$ and $\beta_1(1)=2/3$, thus defining unique K1-model shape parameter values.

It is important to note that although in the temporal domain the K0 response is of SE form, this is not the case for the U model. Transformation of its frequency response to that domain leads to a response that involves an effective SE β value of unity in the short-time limit and a decrease reaching $1/3$ only in the long-time limit.[11] Although both the K0 and U models can be used to fit the same data set, the U model is not only better justified theoretically, but it generally leads to better fits, even for limited-range data. Therefore, it should be used for fitting in place of the K0.

iii. Topological and conclusions. A recent treatment of the motion of ions of a single type in homogeneous materials makes use of physically based topological considerations,[11] not to be confused with geometrical ones. The analysis starts with the recognition that a forcing electric field present between two charged plane-parallel electrodes induces a uniaxially anisotropic local dynamical metric. Within a local polar coordinate frame there is a radial coordinate and $(d-1)$ angular coordinates. For the $d=3$ situation, local motion with respect to the azimuthal coordinate is irrelevant for homogeneous materials, so the effective dimensionality is $d_e=2$, while for streaming motion transverse to the electrodes $d_e=1$. When the approach is applied to temporal stretched-exponential behavior, it leads to just $\beta=d_e/d$, consistent with the present results if $d_e=2$ for the K0 model and $d_e=1$ for the K1 one.

A natural interpretation is that for high frequencies, where hopping motion is local, both models should lead to a limiting slope of $2/3$, as observed for both synthetic and experimental data. The motion of the charges at very low frequencies should be of streaming one-dimensional character, consistent with the U-model value of $\beta_1=1/3$ and with the observation that the synthetic U-model frequency response transformed to the time domain to yield $\phi_1(t)$ is not of stretched-exponential character except in the limit of long times where its stretching parameter is indeed $1/3$ (Ref. 11).

The three disparate approaches above all lead to the same unique value of $\beta_1=1/3$ for the U model and to the corresponding K0 value of $\beta_0=2/3$. Although both models involve the same high-frequency limiting slope of $2/3$, their responses are different except in the extreme high-frequency region, and one generally finds that U-model fits of appropriate experimental data are much better than K0 ones with β_0 fixed at $2/3$ or free to vary, as demonstrated later.

b. Consequences of the $\beta_1=1/3$ requirement and the BNN relation. Now when one sets β_1 fixed at $1/3$ in the K1 model of Eqs. (2) and (4) to obtain the U response model, one finds that $\varepsilon_{C1\infty}=6\varepsilon_{Ma}$, $\varepsilon_{C10}=60\varepsilon_{Ma}$, and so $\Delta\varepsilon_{C1}\equiv\varepsilon_{C10}-\varepsilon_{C1\infty}$

TABLE I. The U row is that for exact scaled U-model data. Rows A–D: $\rho(\omega)$-level U-model CNLS fits to materials with different temperatures and ionic concentrations. The K0 row involves real-part CK0 fitting results of the scaled U-model data, and MA stands for mixed alkali. All fits used modulus weighting (MWT) except those of rows A and K0, where proportional weighting (PWT) was used (Ref. 22). Here $100S_F$ is the percentage value of the relative standard deviation of a fit, and the last column lists its value for fits of the scaled and subtracted data to the U-model hopping response.

Type/Ref.	Material	T (K)	$100S_F$	$10^{-7}\rho_0$ (Ω cm)	$10^{-7}\tau_o$ (s)	$\varepsilon_{C1\infty}$	$\varepsilon_{D\infty}$	$100\overline{S_F}$ or $[\beta_0]$
U	Scaled master: UM			10^{-7}	10^{7}	6	0	
A/35	$0.5Li•0.5La•TiO_3$	179	0.98	6.25	233	25.27	65.01	1.65
B/35	$0.5Li•0.5La•TiO_3$	225	0.42	0.018	0.0467	17.72	80.13	1.29
C/23	$0.2K_2O•0.8GeO_2$	414	1.13	22.8	87.4	2.60	9.29	1.68
D/23	$0.02K_2O•0.98GeO_2$	602	0.45	24.8	2.82	0.077	9.51	1.99
K0	Fit $\sigma'(\overline{\nu})$ UM data		7.4	9.4×10^{-8}	1.6×10^{8}	6.13		[0.638]
MA/2	$0.3(0.6Na_2O•0.4Li_2O)$ $+0.7B_2O_3$			Scaled to $\sigma'(\overline{\nu})$ UM data				

$=54\varepsilon_{Ma}=\Delta\varepsilon$, since $\varepsilon_{D\infty}$ subtracts out from the experimental $\Delta\varepsilon\equiv\varepsilon_0-\varepsilon_\infty$, one of the virtues of using $\Delta\varepsilon$ rather than either of its two components. In addition, if one defines $\varepsilon''_{C1S}(\omega)\equiv\varepsilon''_{C1}(\omega)-(\sigma_0/\omega\varepsilon_V)$, then the resulting dielectric loss arising from charge motion rather than from dipolar dispersion involves a peak response at $\nu_p\equiv\omega_p/2\pi\cong0.011\,22/2\pi\tau_o$, with $\varepsilon''_{C1S}(\omega_p)\cong14.405\varepsilon_{Ma}$ for the peak value.

An empirical expression that has been of considerable importance in the past is that of Barton,[31] Nakjima,[32] and Namikawa,[33] commonly known as the BNN relation,

$$\sigma_0=p\varepsilon_V\Delta\varepsilon\omega_p, \tag{6}$$

where p is a numerical constant of order 1 and ω_p is the radial frequency dielectric loss peak, only equal to the value listed above for the U model. For that model, however, it follows that $p=1/(0.011\,22\times54)\cong1.65$, a universal value for all conductive-system data that are well fitted by the U model.

Figure 3 in Ref. 3 is a log-log BNN-related plot that indicates that most estimates of p are close to the above value, a satisfying result in view of the usual uncertainties associated with estimates of $\Delta\varepsilon$ and ω_p from experimental data. Although Porto *et al.*[34] have recently questioned the applicability of the BNN relation under changes in charge carrier concentration, excellent U-model fittings for wide concentration variation[7] and the results discussed below show that estimates of p from such fits confirm the 1.65 value. Thus, it will usually be appropriate in future to replace the BNN relation by any of those listed above that connect effective dielectric quantities, such as $\varepsilon_{C1\infty}$, to ε_{Ma}.

III. FITTING AND SCALING RESULTS FOR THE U MODEL

When one has available an excellent fitting model applicable for a particular experimental and material domain, there is no need for scaling since data fitting with such a model leads to explicit parameter estimates and thus to more information than does the development of a master scaling model. Although the U model is thus superior to scaling within its domain of applicability, it is instructive to discuss the scaling parameters following from it and to show their applicability for data that include variations of both temperature and relative ionic concentration x_c. For this purpose, data for the following materials will be used, as listed in Table I: $0.5Li\cdot0.5La\cdot TiO_3$ (Ref. 35), $x_cK_2O\cdot(1-x_c)GeO_2$ (Ref. 23), and $0.3(0.6Na_2O\cdot0.4Li_2O)+0.7B_2O_3$ (Ref. 2). The first material is a polycrystalline fast-ionic Li^+ conductor, the second is a homogeneous glass with mobile potassium ions, and the third is a mixed-alkali borate glass with mobile sodium and lithium ions.

A. Scaling possibilities and limitations

Before presenting fitting and scaling results for these materials, it is desirable to consider scaling approaches. It has been customary to write a general scaling relation in the form

$$\sigma'(\omega)/\sigma_0\equiv\rho_0\sigma'(\omega)=F'(\omega\tau_S)\equiv F'(\nu/\nu_S), \tag{7}$$

where the left-hand parts refer to data and the right-hand ones to a fitting model, and $\nu_S\equiv1/(2\pi\tau_S)$ is the scaling frequency. The essence of good scaling then involves choosing appropriate ν_S scaling values. Usually, no fitting is actually carried out, and an equation such as Eq. (7) is merely written to define the type of scaling to be used for $\sigma'(\omega)$ data. Various explicit choices for ν_S and discussions of the historical background of scaling appear in Refs. 2, 3, 6, and 34. Here, scaling will be carried out employing a fully complex version of Eq. (7) for fitting, one that may be used to fit complex data at any immittance level and may include nonhopping processes.

Of the many past choices for ν_S, we here consider only those of Sidebottom,[5] Dyre and Schrøder,[3] Macdonald,[6] and Roling and Martiny.[2] The first two are essentially equivalent, are both related to the BNN relation, and when expressed in terms of ε_{Ma} are $\nu_S\equiv(\varepsilon_{Ma}/\Delta\varepsilon)\tau_o^{-1}$ and $\nu_S\equiv(\varepsilon_{Ma}/\Delta\varepsilon)/(2\pi\tau_o)$, respectively. For the U model, where τ_S becomes the explicit characteristic response time of the model, τ_o, estimated from data fitting, these results lead to $\nu_S=0.0185/\tau_o$

and $\nu_S = 0.00295/\tau_o$, respectively. In contrast, the earlier work of the author[6] involved just the τ_o quantity derived from CMF fits of the K1 model. For the U model, that result becomes $\nu_S \equiv 1/(2\pi\tau_o) = 0.1592/\tau_o$. Finally, Roling and Martiny set $\nu_S \equiv \nu_p$, where ν_p is the frequency at the peak of the mobile-charge dielectric loss response, discussed in Sec. II B. For the U model, the frequency of the $\varepsilon''_{C1S}(\omega_p)$ peak is $\nu_p = 0.001\,786/\tau_o$, a factor of exactly the U-model BNN p value of 1.65 smaller than the Dyre-Schrøder result.

The differences in the numerical values of the numerators of the expressions for all of the above scaling quantities are not significant for scaling, so they are all equivalent in this sense. Nevertheless, the choice of a proper value of τ_o is of the greatest importance for good scaling. Note, however, that since $\Delta\varepsilon$ and ν_p may be directly estimated from experimental data without fitting, a good estimate of τ_o is not actually necessary to form a scaling value of ν_S when a value of σ_0 is available, also necessary for scaling of $\sigma'(\omega)$ itself.

But consider the following: the estimation of $\Delta\varepsilon$ from data requires separate estimated values of both ε_0 and ε_∞. Estimation of both of these quantities, especially that of ε_0, is rendered uncertain by the usual presence of electrode effects, as demonstrated in the next section; in addition, the data often do not extend to high enough frequencies to yield a good estimate of ε_∞. Further, estimation of $\nu_S \equiv \nu_p$ requires subtraction using a good estimate of σ_0 and then the determination of the frequency of the peak of a curve that usually varies slowly in the neighbourhood of the peak, again an inherently inaccurate process for ordinary experimental data.

B. U-model fitting

The above discussion shows that the usual determination of scaling factors may depend on the use of only one or two points of the data, rendering the results uncertain. On the other hand, CNLS estimation of values of σ_0, τ_o, and $\varepsilon_{C1\infty}$ from U-model fitting makes use of all the data in an optimum way, also provides an estimate of $\varepsilon_{D\infty}$, and allows electrode effects to be adequately accounted for as part of the fitting. Therefore, scaling with values of these quantities so estimated is much more appropriate than are other approaches. Let us define the resulting scaled variables as $\overline{\sigma} \equiv \sigma/\sigma_0$ and $\overline{\nu} \equiv \omega\tau_o \equiv \overline{\omega} \equiv \nu/\nu_S$, where $\nu_S \equiv 1/(2\pi\tau_o)$.

Various fitting results are presented in Table I. The U line in the table involves only the K1-model response with β_1 fixed at a value of $1/3$ and the other two parameters each having their scaled values of 1. When, in addition, ε_V is also set to the scaled value of 1, then, from Eq. (3), $\overline{\varepsilon}_{C1\infty} = 6$. All fits of experimental data shown here also used the U model with an extra free parameter to estimate $\varepsilon_{D\infty}$ and usually with additional free parameters (not shown in the table) to account for electrode polarization effects. No such series parameters were needed or could be reliably estimated for the fit of row C, but they were found necessary for all the other fits in order to obtain best overall fits and best bulk parameter estimates. For the fit of row A, a series constant-phase distributed element, the SCPE, defined at the admittance level as $\sigma_{SC} \equiv \varepsilon_V A_{SC}(i\omega)^{\gamma_{SC}}$ with $0 \leqslant \gamma_{SC} \leqslant 1$ (yielding complete blocking when $\gamma_{SC} = 1$), was needed with $\gamma_{SC} \simeq 0.89$. Although inclusion of only a SCPE was found to yield a good fit for the row-B data, the better results shown in the table included a SCPE with a capacitor in parallel, all in series with a completely blocking capacitor.[7,9,10] For the polycrystalline material of rows A and B, the data did not extend to low enough frequencies to allow one to entirely rule out grain-boundary effects. Finally for row D, although again a reasonable fit was obtained on including a SCPE in the composite fitting model, a better fit of the table was found by replacing it by an additional K1 model with its β_1 parameter also fixed at $1/3$.

Other fits of the present data using the K1 model with β_1 free to vary led to estimates of it that were, as usual, very close to $1/3$. See also the fitting results of Refs. 7, 9, and 11 for results for other materials. Even when the relative standard deviation S_F of one of these fits with β_1 free was slightly smaller than that obtained with it fixed at $1/3$, the relative standard deviations of the free parameters were usually smaller than those with it free, indicating a more significant fit. It is also worth emphasizing that comparison of the τ_o estimates for the two types of fit show that they are far less stable than those of β_1 since a small change in the estimate of the latter results in an appreciable change in the corresponding τ_o estimate.

The results shown in the A, B, C, and D rows in the table are consistent with earlier results for different materials where K1-model data fits of the present kind led to $\beta_1 \cong 1/3$ estimates that were nearly independent of both temperature and ionic concentration, making it reasonable to use the fixed value of $\beta_1 = 1/3$ in the present work.[6–11] It is worth noting, however, that the A- and B-row estimates of $\varepsilon_{C1\infty}$ are not exactly proportional here to $1/T$, as expected from Eq. (4) and from earlier work.[7] This discrepancy may be associated with the large role that electrode effects play in the present data, as indicated in the response curves presented below. Fitting results for the data of the mixed-alkali (MA) material listed in the final row of the table is discussed in Sec. III C.

The K0-row results in the table involved real-part $\overline{\sigma'}$ fitting except the listed $\overline{\varepsilon}_{C1\infty}$ value where full complex-data fitting was used. Such fitting necessarily used both the K0 model and a free dielectric-constant ε_x parameter to estimate the $\overline{\varepsilon}_{C1\infty} = 6$ present in the U-model scaled data. The scaled $\overline{\sigma'}(\overline{\nu})$ U-model data, designated UM, extended up to a maximum value of $\overline{\nu} = 10^5$ where the final n slope was about 0.664. This data set was fitted by the real-part K0 model using nonlinear least squares. The last column in the K0 row shows its β_0 estimate in square brackets. For much experimental data where $\overline{\sigma'}(\overline{\nu})$ is no larger than 10^2 to 10^3, CK1-model fitting still leads to $\beta_1 \simeq 1/3$ estimates, but CK0 fitting yields $0.5 < \beta_0 < 0.6$, even though separate power-law fitting of the bulk part of the $\sigma'(\omega)$ data at the high-frequency end usually results in n estimates much closer to $2/3$. Note that although the present CK0-model fit of the virtually exact K1 scaled synthetic data leads to a value of $\varepsilon_{C1\infty} = \overline{\varepsilon}_{C1\infty}$ reasonably close to the exact value of 6, the estimate of $\overline{\tau}_o$ is about 16 rather than 1. Such a larger value than that for K1-model fits is characteristic of K0 fits. Because of the importance of the K0 model to the K1 one, results of fitting the UM data of row 1 of the table using the K0 model with various weight-

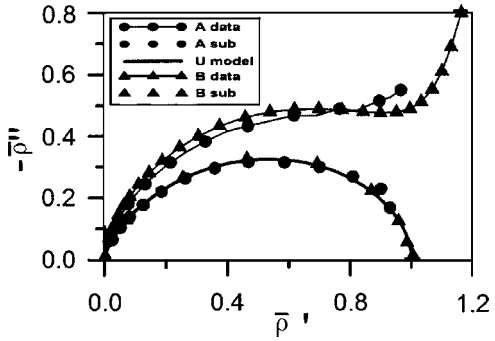

FIG. 1. Complex-plane resistivity plots of scaled data for the A ($T=179$ K) and B ($T=225$ K) rows of Table I, before and after subtraction of all nonhopping contributions and including comparison of the latter results with the exact U-model hopping response.

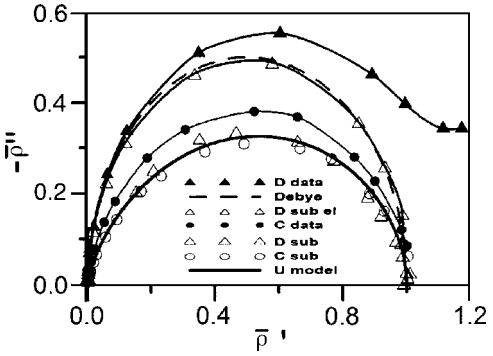

FIG. 2. Stretched complex-plane resistivity plots of scaled variable-concentration data for the C and D rows of Table I, before and after subtraction of all nonhopping contributions for the C data (denoted "C sub") and separate subtractions of electrode effects ("sub el" points) and then of $\varepsilon_{D\infty}$ effects for the D data (denoted "D sub"). The sub el results are compared with pure Debye response and the others with the exact U-model dispersive response.

ing choices are presented and discussed at the end of Sec. III.

Finally, the other quantities in the last column of the table are percentage S_F values for fits of each set of A–D data after subtracting the effects of estimated $\varepsilon_{D\infty}$ and electrode polarization parameters from the original data and then fitting the subtracted results to the scaled U model. As expected, such subtraction of comparable quantities leads to less accurate fits than those involving the full data because it involves the subtraction of nearly equally large quantities to find their small differences. Nevertheless, the two parameter estimates of the model were very close to the exact U-model data values of unity for all four fits of subtracted data.

C. U-model scaling

Complex-plane plots of resistivity data are particularly useful in showing low-frequency electrode effects when present. In order to compare curves for different materials and conditions, all the figures presented here involve data scaled as above using ρ_0 and τ_0 values estimated from the unscaled U-model fits of Table I. Figure 1 presents such results for the A and B material listed in the table. In order to maximize clarity, not all points used in fitting are included in this and the other figures and in none does the size of a data symbol indicate its error bar. In Fig. 1 only about half of the data points are plotted, and, in addition, for the B data the right-hand spur extending to over 1.3 for the actual fitting was cut off as shown. No such cutoff was applied for the A results.

The figure shows that the original (scaled) data lines for the two temperatures are similar for the high-frequency response region, but begin to diverge at the lowest frequencies. The remaining two curves are those for data from which the effects of $\varepsilon_{D\infty}$ and electrode polarization have been subtracted before scaling, a simple procedure after LEVM fitting. It is clear that in the present representation the contributions to the overall frequency response from nonhopping $\varepsilon_{D\infty}$ and series electrode effects dominate the dispersive U-model hopping ones except at the high-frequency end of the curves. Further, we see that the remaining hopping points, identified by "sub" in the figure, fall closely on the U-model master-curve solid line, although those for the A situation show a bit more deviation than do the B ones.

It is particularly important to emphasize that, to the degree that the nonhopping effects were adequately estimated by the fit of the full data, the hopping response shown here does not consist of points fitted to the master curve, but instead it represents the best *hopping-data* estimates obtained from the fits of the full data. The excellent agreement of the hopping points with the exact U-model master curve for both temperatures shows not only that the present scaling is appropriate, but that the hopping response is indeed very well described by the U model and its restriction to $\beta_1=1/3$. As we shall see, these conclusions are further confirmed by the results shown in the subsequent figures. Fitting with a composite model to allow the nonhopping contributions to the full response to be subtracted does not guarantee that the resulting data points will lie close to the U-model hopping curve. That they actually do so is confirmation that the U model represents the dispersive hopping part of the response adequately.

Figure 2 shows a more stringent fitting situation, one where the unscaled dispersive part of the response is much smaller for the low-concentration D condition than that for the C one. Here, in order to maximize resolution and clarity, the *y*-axis-scale unit length is made greater than the *x*-axis one, so this is not quite a traditional complex-plane plot. Low-frequency electrode effects are somewhat less apparent for the present data than are those of Fig. 1, and the differences between the original-data curves and those representing only hopping arise primarily from the relative sizes of the dispersive contributions and those associated with the values of ρ_0 and $\varepsilon_{D\infty}$. As the limit of zero concentration of mobile ions is approached, simple nondispersive Debye relaxation behavior stemming entirely from ρ_0 and $\varepsilon_{D\infty}$ becomes more and more dominant in the data, as discussed in Sec. II B 2 a and demonstrated in detail below.

The second curve from the top of Fig. 2 shows scaled Debye response as a dashed line. Just below it appears the D-material points denoted "sub el" obtained after subtraction of electrode effects from the top D-data curve. The "sub el" points are exceptionally close indeed to the Debye response

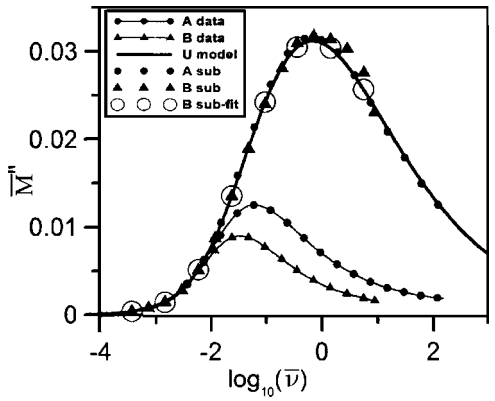

FIG. 3. Scaled $\log_{10}$ frequency response of scaled M'' A and B data before and after subtraction of all nonhopping contributions and including comparison of the latter results with the exact U-model hopping response. In addition, the open circles show the results of fitting the noisy subtracted B data with the U model.

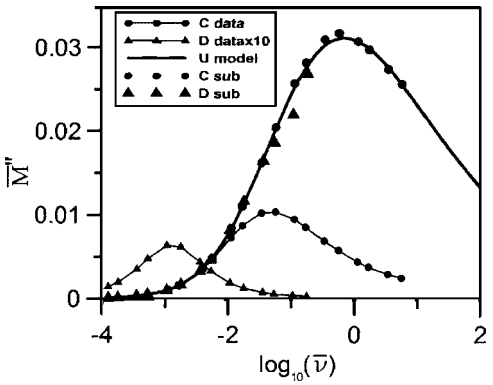

FIG. 4. Scaled $\log_{10}$ frequency response of scaled M'' C and D data before and after subtraction of all nonhopping contributions and including comparison of the latter results with the exact U-model hopping response.

curve here. When the effect of $\varepsilon_{D\infty}$ is then subtracted from these points, however, the resulting D-material bulk dispersion points lie close to the U-model scaled response, but show some scatter arising from stringent subtraction effects. Without such subtraction, however, the resulting original modulus formalism approach leads to a β_1 estimate of about 0.9 instead of 1/3 (Refs. 6, 7, and 23). Because the C data set involves appreciably smaller electrode effects relative to dispersion effects than does the D data, its points after all subtractions lie somewhat closer to the U-model master curve than do the D ones, but their final dispersive hopping responses still show some scatter. Nevertheless, it is clear that both the C and D results scale to the U-model data curve.

Figure 3 presents scaled frequency-response results at the modulus level for the A and B situations. The scaled master curve and the subtracted points all lie appreciably above the original data points primarily because of the subtraction of the effects of $\varepsilon_{D\infty}$ (Refs. 6 and 9). The dispersive B points are poorer, however, than the A ones in the high-frequency region past the peak because electrode effects dominated the former data more than the latter, resulting in greater subtraction errors. Nevertheless, when the somewhat irregular B data points are fitted to the master curve with CNLS, the resulting open-circle points fit excellently.

Figure 4 shows similar results for the C and D material. Note that even with a magnification factor of 10 the original D data curve is appreciably smaller than the corresponding C one, resulting in greater deviations of the D dispersion points from the master curve than for the C points. Nevertheless, the results shown in Figs. 3 and 4 verify both the scaling approach and the appropriateness of the U fitting model.

In Fig. 5, a traditional log-log scaling plot involving scaled σ' and scaled frequency is presented for all four fits included in Table I. In addition, a curve for a mixed-alkali material with two types of mobile ions is included.[2] This curve was scaled to agree with the present master curve at its highest point, and it is evident that it then does not agree well with the single-ion U response curve, particularly in the low-frequency region where dispersion is just beginning to be evident.

The plots in Fig. 5 of the scaled data and those in the magnified inset show appreciable electrode-polarization deviations from the master curve at low frequencies for all the data points, but note particularly the deviations appearing at high frequencies for the A data. The slope of this curve is increasing and reaches a value of about 0.77 at its highest point, in full agreement with prior work on non-negligible high-frequency electrode effects.[8,36] It is thus evident that electrode polarization can be important even at high frequencies where it may sometimes be erroneously identified as arising from nearly constant loss processes.[8,36,37]

In contrast, Fig. 6 shows scaled and fitted results for the dispersive-response parts of the A, B, C, and D data sets. Symbols of different sizes have been used to allow easy identification of the various responses. Although, as one would expect, the present scaling is limited only by the accuracy of the estimation of the scaling parameters from the original CNLS fits and is certainly near optimum, it is particularly gratifying that the estimated dispersive data points fit the master curve so well, thus verifying the appropriateness of the U model for these data sets. In the past, scaling

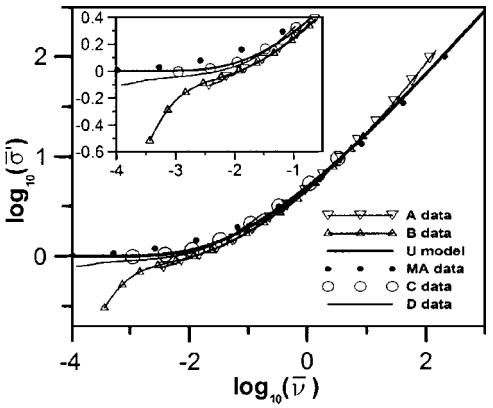

FIG. 5. Log-log scaled frequency response of scaled σ' A–D data sets, including comparison with the exact U-model hopping response. The solid-circle points are for the mixed-alkali data identified in Table I. In addition, the low-frequency parts of the responses are shown with higher resolution in the inset graph.

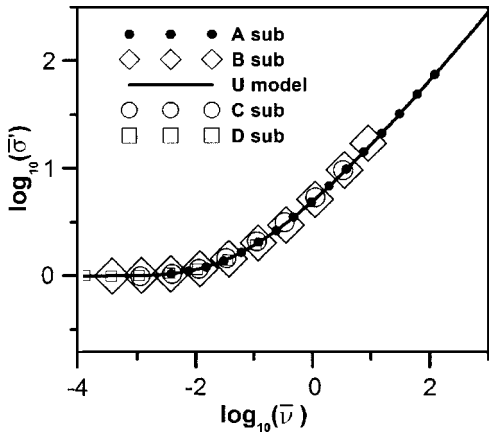

FIG. 6. Log-log scaled frequency response of scaled σ' A–D data sets fitted to the U-model master curve after subtraction of electrode-polarization contributions.

has not usually been attempted for data that involve significant electrode polarization effects, but the present results show that this need not be a limitation, and, as well, it is clear that scaling is unnecessary except to allow comparison of plots for different situations. In most cases, one only need carry out CNLS fits of available data sets to obtain maximum information from them.

The K0 model, through its normalized form $I_{01}(\omega)$, is at the heart of the K1 model, as shown in Eq. (2), and the U model is just the K1 one with β_1 fixed at the theoretically appropriate value of $1/3$. Therefore, the differences between the frequency responses of the U model and the CK0 one are both interesting and important both theoretically and experimentally. Some of these differences are illustrated by the synthetic-data results shown in Figs. 7–9 and indicate under what conditions the CK0 model leads to a high-frequency-limiting slope of $2/3$ so that $\beta_0+\beta_1=1$. Here, exact U-model scaled data, extending to high relative frequencies, is fitted in various ways by the CK0 model. Modulus weighting (MWT), only appropriate for CNLS fitting,[22] led to somewhat better CNLS fits and smaller estimated parameter standard deviations here than did proportional weighting (PWT).

Complex plane resistivity plots such as that of Fig. 7 are particularly useful in emphasizing low-frequency ($\bar{\nu}\leqslant 1$) response, but do not show details of high-frequency behavior well. As is evident, however, there are considerable low-to-midfrequency differences between the U-model response and that of the CK0 with β_0 fixed at $2/3$, ones that appear even though their high-frequency $\bar{\sigma}'$ limiting responses are the same. Figure 8 shows, as expected, that the relative residuals for the two CNLS CK0 fits of Fig. 7 are largest in the lower-frequency regions and those for $\bar{\sigma}'$ become very small at high frequencies as $\bar{\sigma}'$ itself becomes very large. But a plot like this does not indicate how the actual slopes of $\bar{\sigma}'$ vary with frequency for the various situations considered.

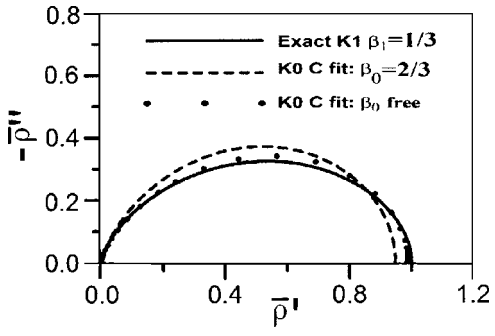

FIG. 7. Complex-resistivity-plane plots of the exact K1 model response with $\beta_1=1/3$ (U-model) and CK0-model fits of the K1 data in complex form (C fits with MWT). With β_0 free to vary, its estimated value was about 0.57.

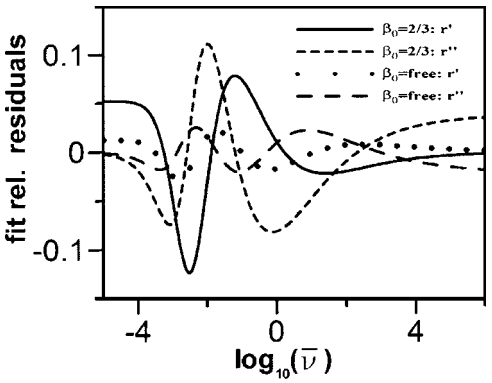

FIG. 8. Real and imaginary relative residuals vs scaled $\log_{10}$ scaled frequency for the two CK0 CNLS fits of Fig. 7.

Therefore, log-log slopes of $\bar{\sigma}'$ versus scaled frequency are presented in Fig. 9. Most noteworthy is the failure of the CNLS CK0 modulus-weighting fit with β_0 free to lead to a value close to $2/3$ even when fitting data for which the maximum value of $\bar{\sigma}'$ is as large as 10^5. When only the $\bar{\sigma}'$ part of the data is fitted, however, the results for PWT, also shown in the K0 row of Table I, yield a limiting slope much closer to $2/3$. PWT weighs all points proportionately, but unity weighting (UWT) emphasizes the largest part most, and although its largest slope value here is about 0.665, it involves the worst estimate of $\bar{\rho}_0$ for all the fits shown. The best estimate of this quantity, 0.987, is that for the complex fit with β_0 free. Complex CK0 fits using PWT or UWT also lead to estimates of β_0 much closer to $2/3$ than does MWT, but other free parameters are less well estimated. The present

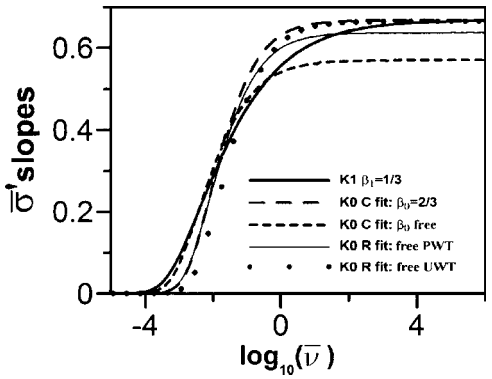

FIG. 9. Scaled real-part conductivity log-log slopes vs $\log_{10}$ scaled frequency for the K1 data and for CK0 complex (C, MWT) and K0 real-part (R) conductivity fits with various weightings.

results show that CK0 fits of U-model data only lead to β_0 estimates close to $2/3$ when weighting is employed that emphasizes the high-frequency part of the data. Similar CK0 fitting of wide-range synthetic K1-model data with $\beta_1=2/3$, appropriate for one-dimensional situations, led to CK0 fits with β_0 close to $1/3$, in agreement with the discussion in Sec. II B 3 a ii.

IV. SUMMARY

The present work shows that for homogeneous materials involving mobile ions of a single type the important β_1 shape parameter of the K1 dispersive frequency-response model has a unique, constant value of $1/3$, resulting in the U model, one whose high-frequency-limiting log-log $\sigma'(\nu)$ slope is $n=2/3$. These results are inapplicable to mixed-alkali situations or to mixed electronic and ionic conduction. For single-ion materials, CNLS fits of frequency-response data with β_1 taken as a free parameter in the K1 model have led to estimates very close to $1/3$. Here it is shown that on fixing β_1 at $1/3$, the U model leads to excellent fits of data independent of temperature and ion-concentration variation, as expected from several different analyses.[6–9,11] Estimates of n at high frequencies by others[25–27,38–40] have led to $n\simeq 2/3$, independent of temperature and ionic concentration over the limited ranges considered, further confirmation of the appropriateness of the U model within its range of applicability.

Scaling, using the U-model fit results of Table I for variable concentration and temperature, was carried out for $\rho(\nu)$, $M''(\nu)$, and $\sigma'(\nu)$ data and resulted in the complex-plane and frequency-response plots of Figs. 1–6. Scaling was initially unsatisfactory for all these data sets because of the influence of nondispersive effects associated with electrode polarization and with $\varepsilon_{D\infty}$. When these effects were subtracted to give best estimates of only the dispersive response, however, scaling of the resulting data was successful and led to data points close to those of the exact scaled U model. Fitting of these data points to this model then yielded scaled parameter values in excellent agreement with those of the model. Even when the best available scaling parameters are used, these results suggest that fitting with a model that takes all processes influencing the data into account may be necessary to yield meaningful scaling comparisons, as it certainly is in order to obtain good estimates of hopping and dielectric parameters from most data. Finally, the results of fits using the K0 model, a crucial precursor of the U model, to U-model data are presented in Figs. 7–9 and show how their responses differ.

ACKNOWLEDGMENTS

The author is grateful to those who provided the data sets used in this study. The many insightful comments and suggestions of Dr. J. C. Phillips have been of great value.

*Electronic address: macd@email.unc.edu

[1] J. C. Phillips, J. Non-Cryst. Solids **172-174**, 98 (1994).
[2] B. Roling and C. Martiny, Phys. Rev. Lett. **85**, 1274 (2000).
[3] J. C. Dyre and T. B. Schrøder, Rev. Mod. Phys. **72**, 873 (2000).
[4] W. K. Lee, J. F. Liu, and A. S. Nowick, Phys. Rev. Lett. **67**, 1559 (1991).
[5] D. L. Sidebottom, Phys. Rev. Lett. **82**, 3653 (1999).
[6] J. R. Macdonald, J. Appl. Phys. **90**, 153 (2001).
[7] J. R. Macdonald, J. Chem. Phys. **116**, 3401 (2002).
[8] J. R. Macdonald, J. Non-Cryst. Solids **307-310**, 913 (2002).
[9] J. R. Macdonald, J. Chem. Phys. **118**, 3258 (2003).
[10] *Impedance Spectroscopy: Theory, Experiment, and Applications*, 2nd ed., edited by E. Barsoukov and J. R. Macdonald (Wiley-Interscience, New Jersey, 2005).
[11] J. R. Macdonald and J. C. Phillips, J. Chem. Phys. **122**, 074510 (2005).
[12] J. C. Phillips, Rep. Prog. Phys. **59**, 1133 (1996).
[13] C. P. Lindsay and G. D. Patterson, J. Chem. Phys. **73**, 3348 (1980).
[14] J. R. Macdonald, Solid State Ionics **150**, 263 (2002).
[15] H. Scher and M. Lax, Phys. Rev. B **7**, 4491 (1973).
[16] J. R. Macdonald, J. Non-Cryst. Solids **212**, 95 (1997).
[17] C. T. Moynihan, L. P. Boesch, and N. L. Laberge, Phys. Chem. Glasses **14**, 122 (1973).
[18] J. R. Macdonald, Phys. Rev. B **63**, 052205 (2001).
[19] M. F. Shlesinger and E. W. Montroll, Proc. Natl. Acad. Sci. U.S.A. **81**, 1280 (1984).
[20] J. Klafter and M. F. Shlesinger, Proc. Natl. Acad. Sci. U.S.A. **83**, 848 (1986).
[21] J. R. Macdonald, J. Appl. Phys. **95**, 1849 (2004).
[22] J. R. Macdonald and L. D. Potter, Jr., Solid State Ionics **23**, 61 (1987); J. R. Macdonald, J. Comput. Phys. **157**, 280 (2000). The newest Windows version, LEVMW, of the comprehensive LEVM fitting and inversion program may be downloaded at no cost from http://www.physics.unc.edu/~macd/. It includes an extensive manual and executable and full source code. More information about LEVM is provided at this www address.
[23] H. Jain and S. Krishnaswami, Solid State Ionics **105**, 129 (1998).
[24] K. L. Ngai, Philos. Mag. B **77**, 187 (1998).
[25] H. Kahnt, Ber. Bunsenges. Phys. Chem. **95**, 1021 (1991).
[26] D. L. Sidebottom, P. F. Green, and R. K. Brow, J. Non-Cryst. Solids **183**, 151 (1995).
[27] D. L. Sidebottom, Phys. Rev. Lett. **83**, 983 (1999).
[28] T. Odagaki and M. Lax, Phys. Rev. Lett. **45**, 847 (1980).
[29] T. Odagaki and M. Lax, Phys. Rev. B **24**, 5284 (1981).
[30] B. Sturman, E. Podivilov, and M. Gorkunov, Phys. Rev. Lett. **91**, 176602 (2003).
[31] J. L. Barton, Verres et Refr.. **20**, 328 (1966).
[32] T. Nakajima, in *Conference on Electrical Insulation and Dielectric Phenomena*, (National Academy of Sciences, Washington, DC, 1972), pp. 168–176.
[33] H. Namikawa, J. Non-Cryst. Solids **18**, 173 (1975).
[34] M. Porto, P. Maass, M. Meyer, A. Bunde, and W. Dieterich, Phys. Rev. B **61**, 6057 (2000).
[35] C. León, J. Santamaria, M. A. Paris, J. Sanz, J. Ibarra, and A.

Varez, J. Non-Cryst. Solids **235-237**, 753 (1998).
[36] J. R. Macdonald, J. Chem. Phys. **115**, 6192 (2001).
[37] J. R. Macdonald, Phys. Rev. B **66**, 064305 (2002).
[38] D. L. Sidebottom, P. F. Green, and R. K. Brow, Phys. Rev. B **51**, 2770 (1995).
[39] L. Murawski and R. J. Barczynski, J. Non-Cryst. Solids **185**, 84 (1995).
[40] D. L. Sidebottom, Phys. Rev. B **61**, 14507 (2000).